JOURNAL OF THERMOPHYSICS AND HEAT TRANSFER
Vol. 23, No. 4, October–December 2009

Technical Notes

Thermal Analysis in a Film Cooling Hole with Thermal Barrier Coating

Dong Hyun Lee,* Kyung Min Kim,† Sangwoo Shin,* and Hyung Hee Cho‡
Yonsei University, Seoul 120-749, Republic of Korea

DOI: 10.2514/1.41341

I. Introduction

FILM cooling and thermal barrier coatings (TBC) are widely used cooling techniques, especially in a gas turbine, which are used to protect a material surface exposed to a high-temperature environment. Increasing the turbine inlet temperature causes the thermal expansion mismatch between the TBC and the substrate, which generates high thermal stresses and thereby TBC delamination as noted in previous reports [1,2]. In addition, TBC delamination has caused thermal cracks on the sides of film cooling holes because temperature difference between regions with and without TBC increased, as reported by the Electric Power Research Institute [3]. Furthermore, the flow temperature on the TBC surface is varied by introducing secondary cooling flow from film cooling holes. Thus, the local thermal loads on the TBC surface with film cooling holes are different from convectional cooling system. However, most previous studies [4–11] of TBC delamination have mainly focused on a convectional cooling system without a film cooling hole, and have also investigated the effects of thermal cycles and thermally grown oxide (TGO) on TBC delamination.

To design hot components such as combustors, vanes, and blades and to predict their lifetime and safety, it is necessary to estimate proper TBC thickness as well as to study the thermal cycles in a film cooling system under an appropriate thermal environment. Thin TBC results in higher metal temperature, whereas thick TBC results in higher TBC temperature, which can be the source of the TBC failure. Therefore, the objective of the present paper is to determine the tolerable TBC thickness at each main hot flow temperature with a film cooling system of normal injection. For the calculation, we conduct thermal analysis using numerical methods [12] and experimental heat transfer data in a nondimensional form (Nusselt number Nu) from the previous studies [13,14]. The test materials of TBC and substrate are yttria-stabilized zirconia (YSZ) coating and IN738-superalloy, respectively. As results, we present maximum temperature and maximum debonding stress values at the edge of cooling holes as a function of two variables, that is, thickness of TBC and temperature of main flow. This work helps to design actual TBC systems and to understand mechanics of interface segregation between TBC and substrate.

II. Numerical Approach and Procedures

To calculate the temperature distributions in the film cooling system, nondimensionalized heat transfer data Nu around a film cooling hole obtained from the previous studies [13,14] are converted into the surface heat transfer coefficients h and adiabatic wall temperature T_{aw} in the scaled-down system. Because the previous experimental system was enlarged from the actual film cooling holes to measure detailed local data, we converted them to actual sizes and flow velocity such as hole diameter D_{eff} of 4.0 mm, total wall thickness (TBC and substrate) of $1.5D_{\text{eff}}$, and main flow velocity of 65.8 m/s using dimensional analysis (scaling laws) with the same blowing rate of 0.57. Wall temperature T_w and wall heat flux q_w were calculated using the converted heat transfer data (h, T_{aw}) and the following heat transfer equations:

$$q_w = h(T_w - T_{\text{aw}}) \tag{1}$$

$$\eta_{\text{aw}} = \frac{T_{\text{aw}} - T_\infty}{T_2 - T_\infty} \tag{2}$$

where the operating and material conditions were considered as follows: coolant flow temperature T_2 of 700 K, main hot gas flow temperature T_∞ from 1100 to 1800 K, TBC thickness of 250∼1500 μm, and substrate thickness of $5.75 \sim 4.5$ mm to keep the total thickness of 6 mm; the materials of the substrate and the TBC are based on IN738 superalloy and YSZ coating, respectively. The material properties are presented in Tables 1 and 2.

Analysis was performed using a commercial code, ANSYS Workbench-11 to calculate the thermal stress. The finite element model and boundary conditions in ANSYS of the film cooling hole are illustrated in Fig. 1. The mapped grid is selected for the mesh construction and the geometry consists of approximately 30,000 elements. The least-mean-square method is used to impose the heat transfer coefficients h and wall adjective flow temperature T_{aw} on the external nodes. As for the boundary conditions (BCs) for constraints, symmetric BCs and BCs for uniform deformation in the x-axis direction due to the existence of additional materials were imposed as shown in Fig. 1. In calculation, the constraints are important because the most stresses are caused by settlements of constraints and thermal effects (arising from temperature changes and differences). After imposing these boundary conditions, stress analysis was conducted to determine the thermal damage in the film cooling system. We have analyzed the thermal stresses, which are proportional to the thermal expansion coefficient α and temperature difference Δt as noted in Eq. (3):

$$\sigma = E\alpha\Delta T \tag{3}$$

For the calculated results, the equivalent or von Mises stress, which is used to predict yielding in ductile materials, for the overall materials is presented. In addition, debonding stress, which acts direction normal to the interface between two materials, is also obtained. The finite element thermal analysis in the present work was conducted as follows:

Step 1) Create a test model using finite elements.

Step 2) Define and impose boundary conditions and the material properties.

Step 3) Calculate temperature distributions induced by conduction in the 3-D test model.

Step 4) Calculate thermal stresses using the temperature distributions and constraint conditions.

Also, to determine the minimum TBC thickness for various main hot gas flow temperatures, we make correlations upon TBC thickness and main hot gas temperature using the response surface method [15]. The maximum material temperature of TBC and substrate as well as the maximum debonding stress are obtained from the correlations at any TBC thickness and main hot gas flow temperature.

Received 30 September 2008; revision received 20 April 2009; accepted for publication 10 May 2009.

*Graduate Student, Department of Mechanical Engineering.
†Research Associate, Department of Mechanical Engineering.
‡Professor, Department of Mechanical Engineering; hhcho@yonsei.ac.kr. Member AIAA.

Table 1 Physical properties of the superalloy

Temperature, °C	Thermal conductivity, W/m°C	Thermal expansion coefficient, μm/m°C	Young's modulus, GPa	Poisson's ratio
100	11.4	11.1	208.8	0.382
300	14.9	13.3	198.6	0.384
500	18.3	14.0	184.6	0.387
700	21.8	14.6	166.9	0.391
900	25.2	15.4	145.5	0.397
1100	28.7	17.3	122.9	0.402

Table 2 Physical properties of the TBC

Temperature, °C	Thermal conductivity, W/m°C	Thermal expansion coefficient, μm/m°C	Young's modulus, GPa	Poisson's ratio
20	1.75	8.5	28.0	0.260
400	1.4	8.9	30.5	0.265
800	1.3	10.1	32.0	0.270
1000	1.25	10.4	32.5	0.275
1200	1.22	10.5	30.1	0.280
1400	1.72	10.5	28.0	0.285

III. Results and Discussion

In general, TBC delamination or cracking depends on various factors such as TBC thickness, main hot gas flow temperature, TGO growth, thermal cycle, thermal shock, microstructure, initial bubble, and mechanical/chemical erosions. In the present study, we considered the TBC thickness and the main hot gas temperature among all other factors because two such factors are the most determinant factors in the beginning of TBC cooling system design. To explain the TBC delamination mode, TBC cracking concept by thermal expansion mismatch (Fig. 2a) and relative concept of its mode (Fig. 2b) are depicted in Fig. 2. The cracking stresses are mainly caused by different thermal properties of TBC and superalloy materials such as thermal conductivity and thermal expansion coefficients at the interface of two materials. That is, the TBC delamination is caused by the debonding stress which acts normal to the interface as shown in Fig. 2b. The debonding stress is the net momentum in the edge of the interface, which is induced by thermal expansion mismatch between TBC and substrate.

Figure 3 shows the temperature distributions near the film cooling hole at $t_{\mathrm{TBC}} = 0.5$ mm (TBC thickness) and $T_m = 1600$ K (hot gas temperature). The temperature distributions on the exposed surface are similar to the film cooling effectiveness in the previous study [14] because the thermal conductivity of TBC is low. The temperature gradients in the x- and y-axis directions are generated by conduction between the hot gas section and cold section as shown in Figs. 3b and 3c. Moreover, the temperature gradient in the side regions of the cooling hole becomes steeper than other regions because of high heat transfer rate. Maximum temperatures of TBC and substrate are 1147.0 and 909.4°C in the upstream region on the external surface, respectively. Minimum temperatures of TBC and substrate are 627.9 and 614.9°C on the inner hole surface in the rear of the injection hole, respectively. In this case, the performance (temperature difference) of TBC is approximately 240°C in the upstream hot region; furthermore, the gradient magnitudes of substrate in x- and y-axis directions are $100 \sim 120$°C and $120 \sim 200$°C, respectively, because the TBC has the low thermal conductivity of approximately 1.3 as listed in Table 2.

The thermal stresses resulting from these temperature distributions are presented in Fig. 4. High thermal stress distributions appear in the interface between TBC and substrate. That is, the maximum vertical (or debonding) stress with a magnitude of 59.24 MPa occurs at the

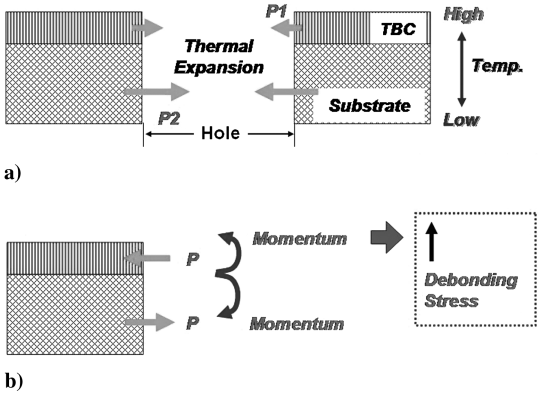

Fig. 2 TBC delamination mode near a film cooling hole: a) concept of TBC cracking by temperature difference, b) definition of debonding stress.

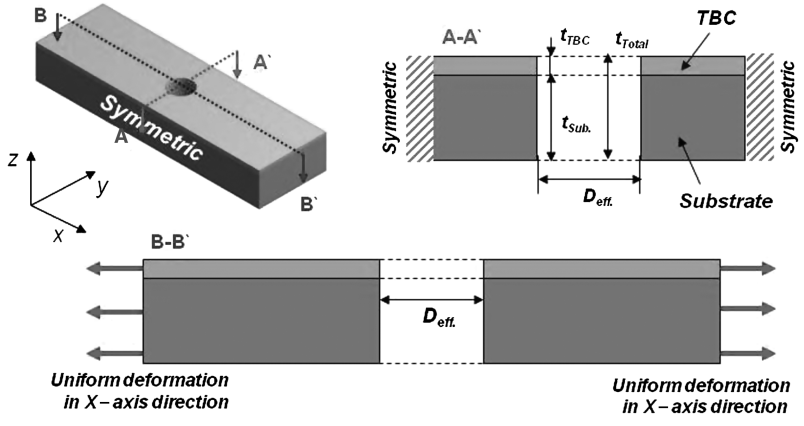

Fig. 1 Geometry and boundary conditions around the film cooling hole.

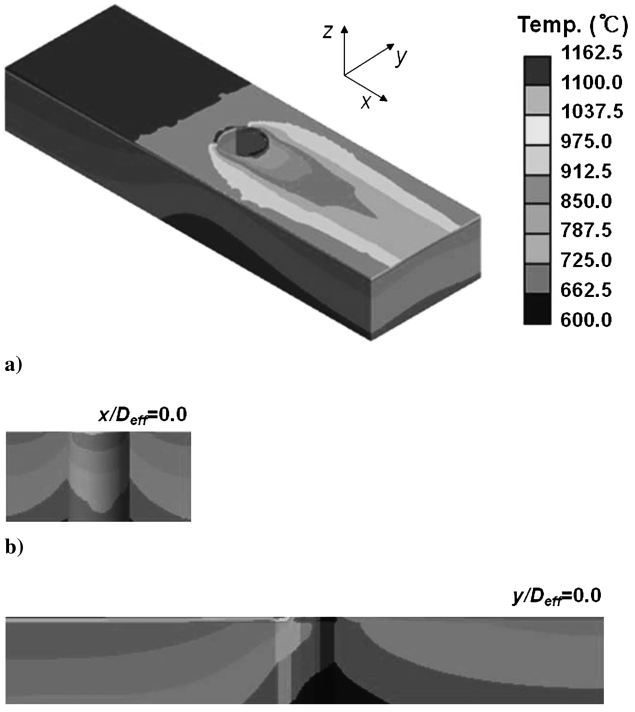

Fig. 3 Temperature distributions near the film cooling hole: a) 3-D view, b) A-A′ cross-sectional view, c) B-B′ cross-sectional view.

edge of the cooling holes due to the highest momentum induced by thermal expansion mismatch (Fig. 4b). Such stress decreases exponentially as being more distant from the cooling hole. These stresses are high enough to yield TBC delamination after numerous thermal cycles with such stress.

Figure 5 shows the maps of maximum temperature of TBC and substrate as a function of the TBC thickness and main hot gas temperature within the design ranges, which are from 0.25 to 1.5 mm and from 827 to 1527°C for t_{TBC} and T_m, respectively. The maximum temperature of both TBC and substrate rises as the main hot gas

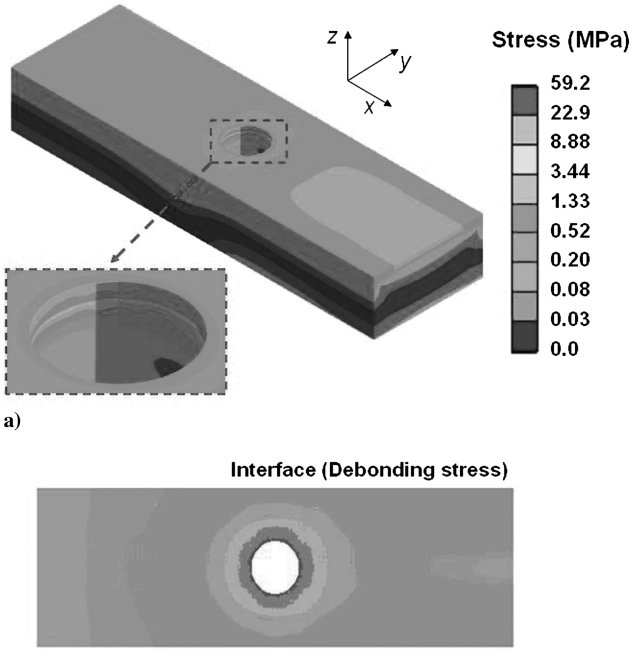

Fig. 4 Stress distributions around the film cooling hole: a) thermal stress distributions, b) debonding stress at the interface.

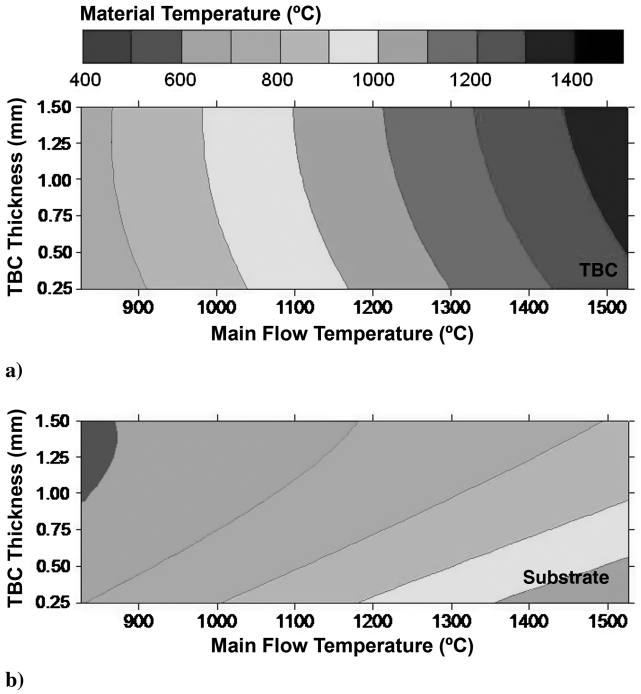

Fig. 5 Maximum material temperature for various TBC thickness and main hot gas temperature: a) highest temperature on TBC, b) highest temperature on substrate.

temperature increases. However, as TBC becomes thicker, the maximum temperature of substrate drops, whereas that of TBC rises. The reduced temperature in TBC material (TBC performance) is calculated using a response surface method. It is deduced as follows:

$$\Delta T = -126.863x_2^2 + 0.279677x_1x_2 + 0.127346x_1 + 103.23x_2 - 142.311 \tag{4}$$

where x_1 is the main hot gas temperature, and x_2 is the TBC thickness.

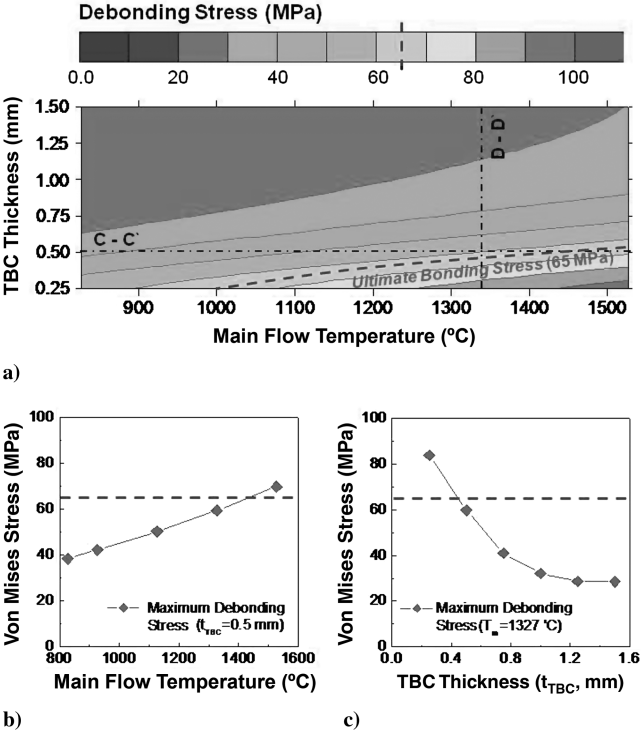

Fig. 6 Maximum debonding stresses: a) contour plot, b) TBC thickness of $t_{\mathrm{TBC}} = 0.5$ mm, c) main hot gas temperature of $T_m = 1327$°C.

Figure 6 shows the maximum debonding stresses σ_{max} calculated from these temperature distributions, which is expressed as follows:

$$\sigma_{max}[\text{MPa}] = 251.32[\exp(-1/x_2)]^2 - 0.097x_1 \exp(-1/x_2) + 0.0569x_1 - 117.56[\exp(-1/x_2)]^2 + 12.909 \quad (5)$$

where x_1 is the main hot gas temperature, and x_2 is the TBC thickness.

Figures 6b and 6c present local data at sections of C-C′ and D-D′ in Fig. 6a. The maximum debonding stress increases as the main hot gas flow temperature increases, whereas the stress decreases as TBC thickness increases. The reason is that the difference in deformation by thermal expansion between TBC and substrate is reduced as TBC thickness increases. In detail, the thick TBC generates a rise in TBC temperature, but a drop in substrate temperature. Thus, the deformations of two materials are similar to each other; in addition, the discrepancy in thermal expansion coefficients between two materials becomes smaller, as presented in Tables 1 and 2.

The dashed line in Fig. 6 indicates the location of the tensile ultimate strength of 65 MPa. That is, TBC will be fractured or cracked when exposed to higher stress than such value. Therefore, in actual design, the TBC thickness at any main hot gas temperature must be carefully considered because both the thin and thick TBC are weak at debonding stress and thermal cycle (or pile of residual stress), respectively. Furthermore, the TBC thickness must be selected using the lower ultimate bonding strength by considering TGO growth, microstructure, etc.

IV. Conclusions

In summary, the present study investigates the effect of TBC thickness and main hot gas temperature on TBC delamination around film cooling holes. The resultant temperature and stresses are calculated using experimental heat transfer data around film cooling holes. As a result, maximum TBC performance and maximum stress values, which are presented as functions of two variables, are shown on the upstream region and at the edges of cooling holes, respectively. Using this method, we will investigate the maximum temperature and debonding stress for the various mechanical properties of TBC in future works.

Acknowledgment

This work was partially supported by the Electric Power Industry Technology Evaluation and Planning Center.

References

[1] Zhu, D., Choi, S. R., and Miller, R. A., "Thermal Fatigue and Fracture Behavior of Ceramic Thermal Barrier Coatings," NASA Rept. No. TM-2001-210816, 2001.

[2] Auerkari, P., Pitkanen, J., Pihkakoski, M., Muurinen, L., Kemppainen, M., and Kangas, P., "Maintenance of Gas Turbines: Impact and Implications for NDT,"*Insight*, Vol. 44, No. 9, 2002, pp. 568–571.

[3] Wan, E., Hong, C., Dewey, R., Bernstein, H., and Norsworthy, D., "Life Management System for Advanced F Class Gas Turbine," Electric Power Research Inst. Rept. No. 1008319, 2005.

[4] Peng, X., and Clarke, D. R., "Piezospectroscopic Analysis of Interface Debonding in Thermal Barrier Coatings," *Journal of the American Ceramic Society*, Vol. 83, No. 5, 2000, pp. 1165–1170.

[5] Chen, X., Hutchinson, J. W., He, M. Y., and Evans, A. G., "On the Propagation and Coalescence of Delamination Cracks in Compressed Coatings: With Application to Thermal Barrier Systems," *Acta Materialia*, Vol. 51, No. 7, 2003, pp. 2017–2030. doi:10.1016/S1359-6454(02)00620-1

[6] Cao, N.-Y., Liu, Y.-F., and Kagawa, Y., "Finite Element Analysis of a Barb Test for Thermal Barrier Coating Delamination Toughness Measurement," *Surface and Coatings Technology*, Vol. 202, No. 13, 2008, pp. 3109–3114. doi:10.1016/j.surfcoat.2007.11.012

[7] Baker, M., Rosler, J., and Heinze, G., "A Parametric Study of the Stress State of Thermal Barrier Coatings Part II: cooling stresses," *Acta Materialia*, Vol. 53, No. 2, 2005, pp. 469–476. doi:10.1016/j.actamat.2004.10.004

[8] Aktaa, J., Sfar, K., and Munz, D., "Assessment of TBC Systems Failure Mechanisms Using a Fracture Mechanics Approach," *Acta Materialia*, Vol. 53, No. 16, 2005, pp. 4399–4413. doi:10.1016/j.actamat.2005.06.003

[9] Busso, E. P., Wright, L., Evans, H. E., McCartney, L. N., Saunders, S. R. J., Osgerby, S., and Nunn, J., "A Physics-Based Life Prediction Methodology for Thermal Barrier Coating Systems," *Acta Materialia*, Vol. 55, No. 5, 2007, pp. 1491–1503. doi:10.1016/j.actamat.2006.10.023

[10] Smialek, J. L., Zhu, D., and Cuy, M. D., "Moisture-Induced Delamination Video of an Oxidized Thermal Barrier Coating," *Scripta Materialia*, Vol. 59, No. 1, 2008, pp. 67–70. doi:10.1016/j.scriptamat.2008.02.055

[11] Faulhaber, S., Mercer, C., Moon, M.-W., Hutchinson, J. W., and Evans, A. G., "Buckling Delamination in Compressed Multilayers on Curved Substrates with Accompanying Ridge Cracks," *Journal of the Mechanics and Physics of Solids*, Vol. 54, No. 5, 2006, pp. 1004–1028. doi:10.1016/j.jmps.2005.11.005

[12] Kim, K. M., Lee, D. H., and Cho, H. H., "Thermal Analysis of a Film Cooling System with Normal Injection Holes Using Experimental Data," *International Journal of Fluid Machinery and Systems*, Vol. 2, No. 1, 2009, pp. 55–60.

[13] Cho, H. H., and Goldstein, R. J., "Heat (Mass) Transfer and Film Cooling Effectiveness with Injection Through Discrete Holes, Part I: Within Holes and on the Back Surface," *Transactions of the ASME: Journal of Turbomachinery*, Vol. 117, No. 3, 1995, pp. 440–450. doi:10.1115/1.2835680

[14] Cho, H. H., and Goldstein, R. J., "Heat (Mass) Transfer and Film Cooling Effectiveness with Injection Through Discrete Holes, Part II: On the Exposed Surface," *Transactions of the ASME: Journal of Turbomachinery*, Vol. 117, No. 3, 1995, pp. 451–460. doi:10.1115/1.2835681

[15] Myers, R. H., *Response Surface Methodology*, 2nd ed., Wiley, Hoboken, NJ, 2002.